Macromolecules

ARTICLE

pubs.acs.org/Macromolecules

Benzobisthiazole-Based Donor−Acceptor Copolymer Semiconductors for Photovoltaic Cells and Highly Stable Field-Effect Transistors

Eilaf Ahmed,[†] Selvam Subramaniyan,[‡] Felix S. Kim,[‡] Hao Xin,[‡] and Samson A. Jenekhe*[,†,‡]

[†]Department of Chemistry and [‡]Department of Chemical Engineering, University of Washington, Seattle, Washington 98195-1750, United States

Supporting Information

ABSTRACT:

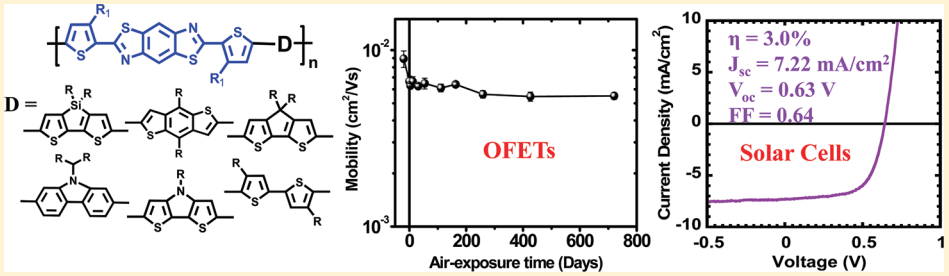

Six new donor−acceptor copolymers based on benzobisthiazole and various donor moieties (dithienosilole, dithienopyrrole, cyclopentadithiophene, carbazole, benzodithiophene, and bithiophene) were synthesized, characterized, and used in field-effect transistors and solar cells. The series of polybenzobisthiazoles with donor−acceptor architecture have optical band gaps of 1.83−2.18 eV, have identical LUMO energy levels (∼−3.3 eV), and have a HOMO energy level that varied from −4.79 eV in PBTDTP to −5.71 eV in PBTHDDT. X-ray diffraction of the polybenzobisthiazole films showed a lamellar crystalline structure with an interlayer *d*-spacing of 1.56 nm in PBTOT to 1.83 nm in PBTDTP and 2.12 nm in PBTHDDT and a short π-stacking distance (0.353−0.378 nm). The highly crystalline nature of the polybenzobisthiazoles facilitated high field-effect carrier mobility (up to 0.011 $cm^2/(V\,s)$), which remained very stable under ambient conditions for 2 years. Bulk heterojunction solar cells made from one of the benzobisthiazole-based copolymers gave a power conversion efficiency of up to 3.0% under 100 mW/cm^2 AM1.5 sunlight illumination in air.

1. INTRODUCTION

Organic semiconductors are of broad interest for applications in electronics and optoelectronics including photovoltaic cells and field-effect transistors.[1−20] Donor−acceptor (D−A) conjugated polymers are among the widely studied organic semiconductors for these applications.[1−5,14−18] By judicious selection of the donor and the acceptor units, the D−A copolymer architecture enables engineering of the electronic structure including the highest occupied molecular orbital (HOMO) and the lowest unoccupied molecular orbital (LUMO) energy levels, the energy band gap and light harvesting properties, and charge transport properties.[1−5,14−18] Indeed, D−A copolymers based on 3-alkylthiophene segments[6−10] and derivatives[11−13] have resulted in field-effect transistors with high carrier mobility[9−18] and solar cells with high efficiency.[3−5] To improve the oxidative and thermal stability of polymer semiconductors in ambient conditions, several strategies have been used, including incorporation of fused aromatic[11−13] or aromatic heterocyclic rings[15−18] and use of alternating donor−acceptor system.[2−5,14−18] Fused aromatic rings such as thienothiophene[12,13] and benzodithiophene[11b] and imine-rich aromatic heterocyclic rings[3c,d,15−18] such as thiazolothiazole,[3a,b,15] 5,5′-bithiazole,[16] and thienopyrazine[3e,f] exemplify this approach. Incorporation of fused cyclic rings can also lead to enhanced intermolecular π-stacking interactions and long-range order.[1−4,12,13]

Because polybenzobisazoles,[20−27] including benzobisthiazole and benzobisoxazole polymers, exhibit a high degree of molecular order, early studies focused on their thermal stability, mechanical properties, and their use as structural materials.[21] Polybenzobisazoles were later developed for application in electronics and optoelectronics.[20,22−27] Benzobisthiazole and benzobisoxazole polymers and small molecules were found to exhibit efficient π-stacking and strong intermolecular interactions in the solid state,[22] leading to thermally robust materials that have high glass transition temperatures (>300−400 °C) and relatively high electron affinity.[20,23−25] They were used in electronic applications including as electron transport materials[23b] in organic light-emitting diodes,[23a] as nonlinear optical materials,[24] and as charge photogeneration materials in xerographic photoreceptors.[25]

Received: May 17, 2011
Revised: August 5, 2011
Published: August 22, 2011

ACS Publications © 2011 American Chemical Society

Chart 1. Molecular Structures of Benzobisthiazole-Based Copolymers

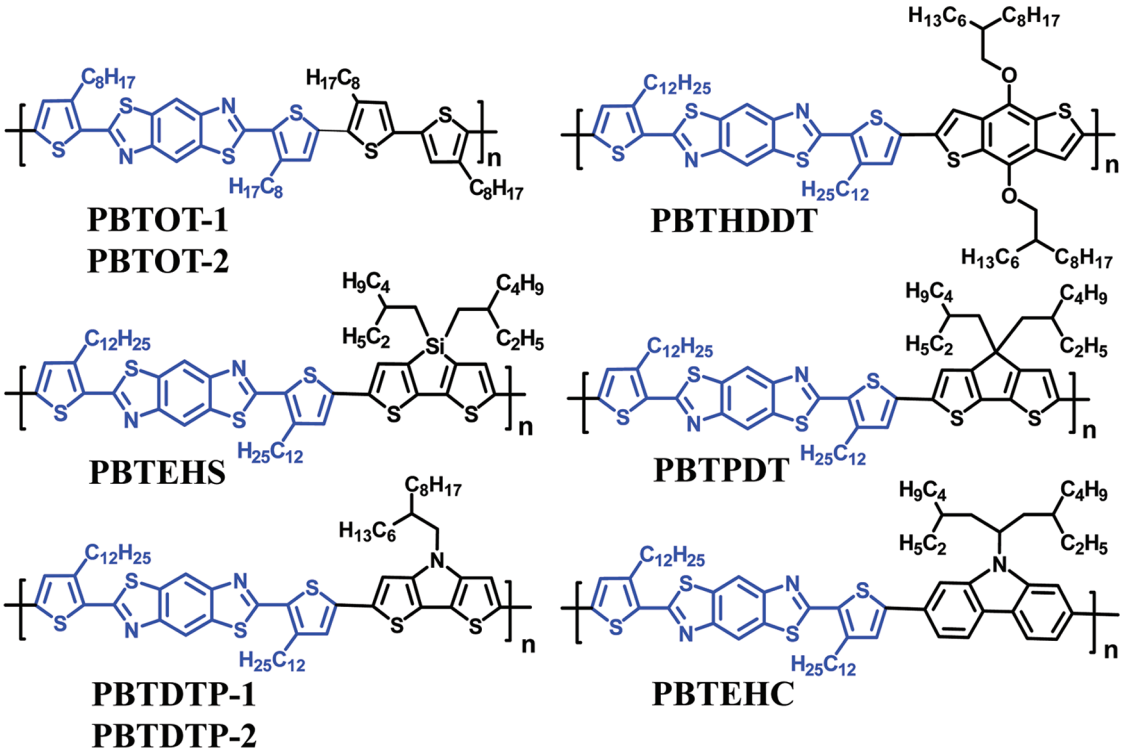

Light-emitting diodes containing polybenzobisthiazole electron transport layer were found to be stable in air for over a period of 10 months.[23b] Studies of poly(*p*-phenylene benzobisthiazole) (PBZT) as an n-channel semiconductor in field-effect transistors were limited by their low carrier mobility.[20] A high electron affinity n-type polymer[19] in a blend with PBZT was needed to facilitate electron injection.[20] Recently, benzobisthiazole small molecules were found to exhibit high carrier mobility in thin film field-effect transistors.[26] However, despite these numerous attractive properties of benzobisthiazole-based polymers and small molecules, their limited solubility in organic solvents has hindered their widespread applications in organic electronics and optoelectronics.[20−26]

In a recent preliminary report,[17] we introduced an alternative synthetic approach that incorporates alkyl side chains into the backbone of benzobisthiazole−oligothiophene D−A copolymers to promote solubility in organic solvents. We found that the new copolymers had enhanced intermolecular interactions and improved oxidative stability, good field-effect charge transport with a carrier mobility of 0.01 $cm^2/(V\ s)$, and promising photovoltaic properties. Indeed, similar benzobisthiazole copolymers were later reported to have a higher mobility of holes ($\mu_h = 0.26\ cm^2/(V\ s)$) and highly stable devices in air for 2 months under relatively high humidity conditions (RH ∼ 30−75%).[18]

In this paper, we report the synthesis and investigation of the morphological, optical, electrochemical, field-effect charge transport, and photovoltaic properties of six D−A copolymer semiconductors based on benzobisthiazole and the durability of the field-effect transistors in ambient air. The molecular structure of the series of benzobisthiazole-based D−A copolymers are shown in Chart 1. High molecular weight benzobisthiazole-based copolymers can easily be obtained via Stille cross-coupling polymerization. The optical band gap of the polybenzobisthiazoles varied from 2.18 to 1.83 eV while the HOMO energy level could be tuned from −4.79 to −5.71 eV by varying the comonomer donor strength. X-ray diffraction on solution-cast films showed that all of the six copolymers are highly crystalline and form a lamellar ordering with a small *d*-spacing (15.6−21.2 Å) and a short π-stacking distance (3.5−3.8 Å). The enhanced molecular packing in the polybenzobisthiazoles gives rise to thermally robust materials with high melting temperatures (290−367 °C). As p-channel materials in OFETs, the benzobisthiazole copolymers had field-effect carrier mobilities of up to 0.011 $cm^2/(V\ s)$ with high on/off current ratio (>10^6). Remarkable stability of the benzobisthiazole-based copolymer in air was observed, and the device performance, including the carrier mobility, on/off current ratio, and threshold voltage, has remained the same for almost 2 years in ambient conditions. Bulk heterojunction solar cells made from the new polybenzobisthiazoles (PBTs) gave power conversion efficiency of up to 3.0% under 100 mW/cm^2 AM1.5 sunlight illumination in ambient conditions.

2. EXPERIMENTAL SECTION

2.1. Materials and Synthetic Procedures. *Materials.* All commercially obtained reagents were used without further purification.

Synthetic Procedures. Compounds **1**,[17] **3**,[14c,5a] 4,4′-dioctyl-5,5′-trimethylstannyl-2,2′-bithiophene,[17] and **5**[5c] were synthesized according to previously reported methods. 2,6-Dibromo-4,4′-bis(2-ethylhexyl)-4*H*-cyclopenta[2,1-*b*:3,4-*b*′]dithiophene and 2,6-dibromo-4,4-bis(2-ethylhexyl) dithieno[3,2-*b*:4,5-*b*′]silole were purchased from Luminescence Technology Corp. and were used without further purification.

2,6-Bis(3-dodecylthiophen-2-yl)benzo[1,2-d;4,5-d′]bisthiazole. A mixture of 2,5-diamino-1,4-benzenedithiol dihydrochloride (4.98 g, 20.4 mmol), 3-dodecylthiophene-2-carboxylaldehyde (20.0 g, 71.4 mmol), and diphenyl phosphate (8 equiv) in 10 mL of toluene was refluxed under

N_2 for 12 h. The reaction mixture was poured into water and extracted with 1,2-dichloromethane (3×). The organic phase was washed with 10% NaOH (3×) and brine, dried with $NaSO_4$, and filtered, and the solvent was evaporated by vacuum. The crude product was purified by column chromatography (5:1 hexane:chloroform) followed by recrystallization from hexane:chloroform mixture to yield a yellow solid (1.3 g, 9%). ESI mode: found $M + 1 = 694.1$; requires 693.15. ^{1}H NMR ($CDCl_3$): δ 8.51 (s, 2H), δ 7.45 (d, 2H), δ 7.06 (d, 2H), δ 3.10 (t, 4H), 1.78 (m, 6H), δ 1.51−1.28 (m, 34H), δ 0.894 (t, 6H).

*2,6-Bis(5-bromo-3-dodecylthiophen-2-yl)benzo[1,2-d;4,5-d′]-bisthiazole (**1**).* 2,6-Bis(3-dodecylthiophen-2-yl)benzo[1,2-*d*;4,5-*d*′]-bisthiazole (1.3 g, 1.88 mmol) was dissovled in 37 mL of 2:1 chloroform:DMF at room temperature in the dark. NBS was dissolved in 5 mL of DMF and was slowly added to the mixture. The mixture was stirred at room temperature for 96 h. The crude product was extracted with chloroform, washed with water, and dried with Na_2SO_4. The crude product was purified by column chromotography using chloroform as the eluent solvent and recrystallized from chloroform to give a yellow solid (1.1 g, 69%). ESI mode: found $M + 1 = 852.1$; requires 850.934. ^{1}H NMR ($CDCl_3$): δ 8.47 (s, 2H), δ 7.01 (s, 2H), δ 3.03 (t, 4H), 1.77−1.73 (m, 6H), δ 1.38−1.33 (m, 34H), δ 0.896 (t, 6H).

*2,6-Bis(5-trimethyltin-3-dodecylthiophen-2-yl)benzo[1,2-d;4,5-d′]-bisthiazole (**2**).* To a solution of 2,6-bis(5-bromo-3-dodecylthiophen-2-yl)benzo[1,2-*d*;4,5-*d*′]bisthiazole (**1**) (350 mg, 0.4 mmol) in 50 mL of THF, 2.5 M solution of *n*-BuLi in hexane (0.41 mL, 1.03 mmol) was added dropwise at −78 °C. The solution was stirred at −78 °C for 2 h, and 1.0 M solution of trimethyltin chloride (1.23 mL, 1.23 mmol) in THF was added in one portion. The solution was warmed to room temperature and stirred overnight. The reaction mixture was poured into 50 mL of water, and 50 mL of ethyl acetate was added. The organic layer was washed twice with 50 mL of water and dried with Na_2SO_4. The organic layer was evaporated, and the product was then dried in a vacuum oven to afford a yellow solid (400 mg, 93% yield). ^{1}H NMR ($CDCl_3$, 300 MHz, ppm): δ 8.47 (s, 2H), 7.08 (s, 2H), 3.07 (t, 4H, 7.5 Hz), 1.76 (s, 4H), 1.26−1.48 (m, 36 H), 0.85−0.87 (m, 6H), 0.42 (s, 18H). ESI mode: found $M + 1 = 1019.6$; requires 1018.76.

*2,6-Di(trimethyltin)-N-(1-hexyldecyl)dithieno[3,2-b:30-d]pyrrole (**4**).* *n*-BuLi (1.43 mL, 3.57 mmol, 2.5 M in hexane) was added into a solution of **3** (690 mg, 1.70 mmol) in THF (50 mL) at −78 °C. The mixture was maintained at this temperature for 1 h, warmed to room temperature for another 15 min, and then recooled to −78 °C. Trimethyltin chloride (750 mg, 3.74 mmol) was added at once, and the mixture was stirred at room temperature overnight. The product was extracted with diethyl ether (3 × 65 mL). The combined organic layers were washed with water and brine (2 × 100 mL) and dried with $MgSO_4$. The solvent was removed under reduced pressure, and the residue was washed with ethanol to afford **3** (850 mg, 69%). ^{1}H NMR ($CDCl_3$, 300 MHz, ppm): δ 7.00 (s, 2H), 4.04 (d, 2H, 7.2 Hz), 2.02 (br, 1H), 1.23−1.29 (m, 24H), 0.86−0.87 (m, 6H), 0.56−0.61 (s, 18H). ESI mode: found $M + 1 = 730.1$; requires 729.3.

*1,5-Bistrimethyltin-4,8-di(2-hexyldecyloxy)benzo[1,2-b:3,4-b]dithiophene (**6**).* To a solution of **5** (1.2 g, 1.81 mmol) in 40 mL of THF, 2.5 M solution of *n*-BuLi in hexane (1.8 mL, 4.52 mmol) was added dropwise at −75 °C under N_2. The solution was stirred at −78 °C for 30 min and warmed to room temperature for 30 min. The mixture was cooled again to −78 °C, 1.0 M solution of trimethyltin chloride (5.43 mL, 5.42 mmol) in THF was added, and the mixture was stirred at room temperature overnight. The resulting mixture was quenched with 50 mL of water, extracted with hexanes, and dried with anhydrous Na_2SO_4. The organic layer was evaporated and dried in vacuum oven to afford **2** as colorless needles (1.4 g, 79%). ^{1}H NMR ($CDCl_3$, 300 MHz, ppm): δ 7.51 (s, 2H), 4.18 (d, 4H, 5.4 Hz), 1.86 (m, 2H), 1.29−1.64 (m, 48H), 0.89−0.90 (s, 12H), 0.44 (s, 18H). ESI mode: found $M + 1 = 997.5$; requires 996.75.

Poly[(4,8-bis(2-hexyldecyl)oxy)benzo[1,2-b:4,5-b′]dithiophene)-2,6-diyl-alt-(2,5-bis(3-dodecylthiophen-2-yl)benzo[1,2-d;4,5-d′]bisthiazole)] (PBTHDDT). A mixture of **1** (350 mg, 0.411 mmol), 4,8-bis(2-hexyldecyl)-oxy)-2,6-bis(trimethyltin)benzo[1,2-*b*:4,5-*b*′]dithiophene) (**6**) (441 mg, 0.411 mmol), tris(dibenzylideneacetone)dipalladium(0) (7.5 mg, 0.0082 mmol), and tris-*o*-tolyphosphine (10.0 mg, 0.033 mmol) in 15 mL of chlorobenzene was refluxed for 72 h. The reaction solution was poured into 200 mL of 5% hydrochloric acid/methanol solution and stirred for 5 h. The filtered solid was subjected to Soxhlet extraction with methanol and hexane for 24 h each. The product was dried in vacuum oven for 12 h and collected as a shiny green solid (484 mg, 86%). ^{1}H NMR ($C_6D_4Cl_2$, 60 °C): δ 8.60−7.25 (m, 6H), 4.44 (m, 4H), 3.21 (s, br, 4H), 1.93−1.00 (m, 108 H). GPC: M_w = 56.7 kDa, M_n = 19.94 kDa, PDI = 2.84.

Poly(2,6-bis(3-octyl-5-(3-octylthiophen-2-yl)thiophen-2-yl)benzo-[1,2-d;4,5-d′]bisthiazole) (PBTOT). A mixture of 2,6-bis(5-bromo-3-octylthiophen-2-yl)benzo[1,2-*d*;4,5-*d*′]bisthiazole[17] (300 mg, 0.406 mmol), 4,4′-dioctyl-5,5′-trimethylstannyl-2,2′-bithiophene[17] (291 mg, 0.406 mmol), tris(dibenzylideneacetone)dipalladium(0) (7.4 mg, 0.00812 mmol), and tris-*o*-tolyphosphine (9.89 mg, 0.0325 mmol) in 12 mL of chlorobenzene was refluxed for 84 h. The reaction solution was poured into 200 mL of 5% hydrochloric acid/methanol solution and stirred for 5 h. The filtered solid was subjected to Soxhlet extraction with methanol and hexane for 24 h each. PBTOT-1 was extracted with chlorofrom to give a shinny green solid (100 mg), and PBTOT-2 (140 mg) was insoluble fraction from chloroform which was dissolved in 1,2-dichlorobenzene and precipitated from methanol (240 mg, 61%). ^{1}H NMR ($CDCl_3$): δ 8.44 (s, 2H), 6.81 (s, br, 4H), 3.03−2.53 (m, 8H), 1.68 (m, 8H), 1.31 (m, 40H), 0.91 (m, 12H). GPC: PBTOT-1: M_w = 15.4 kDa, M_n = 8.06 kDa, PDI = 1.91. PBTOT-2: M_w = 722.0 kDa, M_n = 366.5 kDa, PDI = 1.97.

Poly[(4,4′-bis(2-ethylhexyl)dithieno[3,2-b:2′,3′-d]silole)-2,6-diyl-alt-(2,5-bis(3-dodecylthiophen-2-yl)benzo[1,2-d;4,5-d′]bisthiazole)] (PBTEHS). A mixture of **2** (381 mg, 0.374 mmol), 2,6-dibromo-4,4-bis(2-ethylhexyl)dithieno[3,2-*b*:4,5-*b*′]silole (216 mg, 0.374 mmol), tris(dibenzylideneacetone)dipalladium(0) (6.9 mg, 0.007 54 mmol), and tris-*o*-tolyphosphine (9.1 mg, 0.0299 mmol) in 20 mL of chlorobenzene was refluxed for 72 h. The solution was poured into 200 mL of 5% hydrochloric acid/methanol solution and stirred for 5 h. The filtered solid was subjected to Soxhlet extraction with methanol and hexane for 24 h each. The product was dried in a vacuum oven for 12 h and collected as a dark solid (380 mg, 92%). ^{1}H NMR ($CDCl_3$): δ 8.48 (br, 2H), 7.34−7.31 (br, 4H), 3.06 (m, 8H), 1.81 (br, 8H), 1.30 (br, 50H), 0.91 (br, 18H). GPC: M_w = 19.2 kDa, M_n = 7.82 kDa, PDI = 2.46.

Poly[(4,4′-bis(2-ethylhexyl)-4H-cyclopenta[2,1-b:3,4-b′]dithiophene)-2,6-diyl-alt-(2,5-bis(3-dodecylthiophen-2-yl)benzo[1,2-d;4,5-d′]bisthiazole)] (PBTPDT). A mixture of **2** (414 mg, 0.406 mmol), 2,6-dibromo-4,4′-bis(2-ethylhexyl)-4*H*-cyclopenta[2,1-*b*:3,4-*b*′]dithiophene (228 mg, 0.406 mmol), tris(dibenzylideneacetone)dipalladium(0) (7.4 mg, 0.008 08 mmol), and tris-*o*-tolyphosphine (9.9 mg, 0.0315 mmol) in 6 mL of chlorobenzene was refluxed for 72 h. The reaction solution was poured into 200 mL of 5% hydrochloric acid/methanol solution and stirred for 5 h. The filtered solid was subjected to Soxhlet extraction with methanol and hexane for 24 h each. The product was dried in a vacuum oven for 12 h and collected as a dark solid (381 mg, 86%). ^{1}H NMR ($C_6D_4Cl_2$, 60 °C): δ 8.48 (s, 2H), 7.44−7.27 (m, 4H), 3.16 (s, 4H), 2.12−0.82 (m, 80H). GPC: M_w = 13.9 kDa, M_n = 9.87 kDa, PDI = 1.41.

Poly[(4-(2-hexyldodecyl)-4H-dithieno[3,2-b:2′,3′-d′]pyrrole)-2,6-diyl-alt-(2,5-bis(3-dodecylthiophen-2-yl)benzo[1,2-d;4,5-d′]bisthiazole)] (PBTDTP). A mixture of **1** (210 mg, 0.246 mmol), 4-(2-hexyldodecyl)-2,6-bis(trimethyltin)-4*H*-dithieno[3,2-*b*:2′,3′-*d*′]pyrrole (180 mg, 0.246 mmol), tris(dibenzylideneacetone)dipalladium(0) (4.5 mg, 0.00491 mmol), and tris-*o*-tolyphosphine (6.0 mg, 0.0197 mmol) in 5.4 mL of chlorobenzene

Scheme 1. Synthetic Route to Benzobisthiazole-Based Donor−Acceptor Copolymers

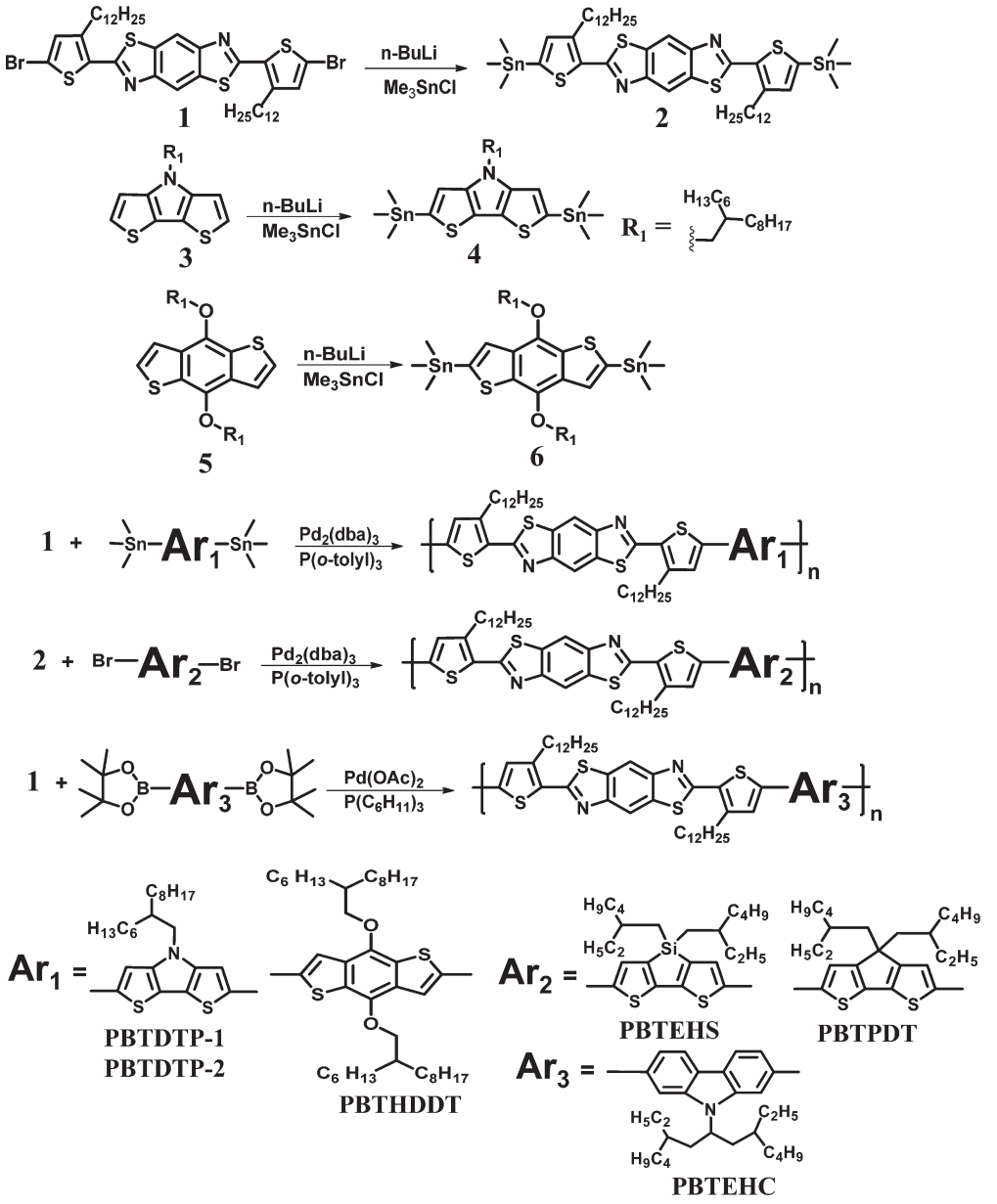

was refluxed for 72 h. The reaction solution was poured into 200 mL of 5% hydrochloric acid/methanol solution and stirred for 5 h. The filtered solid was subjected to Soxhlet extraction with methanol and hexane for 24 h each. PBTDTP-1 was extracted with chlorofrom to give a shinny green solid (68.8 mg), whereas the insoluble fraction PBTDTP-2 (172 mg) remained in the filter paper (241 mg, 90%). ^{1}H NMR ($C_6D_4Cl_2$, 60 °C): δ 8.43−8.17 (m, 4H), 7.30−7.00 (m, 2H), 4.10 (s, br, 2H), 3.18 (s, br, 4H), 1.91−0.98 (m, 77H). GPC: PBTDTP-1: M_w = 32.1 kDa, M_n = 10.3 kDa, PDI = 3.12. PBTDTP-2: M_w = 147.6 kDa, M_n = 52.4 kDa, PDI = 2.82.

Poly[9-(3-ethyl-1-(2-ethylhexyl)heptyl)-9H-carbazole-2,7-diyl-alt-(2,5-bis(3-dodecylthiophen-2-yl)benzo[1,2-d;4,5-d′]bisthiazole)] (PBTEHC). A mixture of **1** (300 mg, 0.353 mmol), 9-[3-ethyl-1-(2-ethylhexyl)heptyl]-2,7-bis(4,4,5,5-tetramethyl-1,3,2-dioxaborolan-2-yl)-9*H*-carbazole (232 mg, 0.353 mmol), palladium(0)(diacetate) (158 mg, 0.00704 mmol), and tricyclohexylphosphine (2.96 mg, 0.0106 mmol) in 6 mL of toluene and 1.5 mL of tetraethylammonium hydroxide was refluxed for 72 h. The reaction solution was poured into 200 mL of 5% hydrochloric acid/methanol solution and stirred for 5 h. The filtered solid was subjected to Soxhlet extraction with methanol and hexane for 24 h each. The product was dried in a vacuum oven for 12 h and collected as a dark solid (233 mg, 60%). ^{1}H NMR ($C_2D_4Cl_2$, 60 °C): δ 8.53 (br, 2H), 8.12 (br, 2H), 7.93 (br, 2H), 7.70 (br, 2H), 7.02 (br, 2H), 4.93 (m, 1H), 3.16 (br, 4H), 2.48 (br, 4H), 1.88−0.77 (m, 76H). GPC: M_w = 11.4 kDa, M_n = 6.8 kDa, PDI = 1.68.

2.2. Characterization. ^{1}H NMR spectra were recorded on a Bruker AV300 at 300 MHz or DRX 499 MHz using $CDCl_3$, $C_6D_4Cl_2$, or $C_2D_4Cl_2$ as the solvent. Mass spectra were obtained from the Bruker Esquire LC/ion trap mass spectrometer. Differential scanning calorimetry (DSC) analysis was performed on a TA Instruments Q100 under N_2 at a heating rate of 10 °C/min. Second-heating DSC scans are reported for PBTOT-1 and PBTOT-2; first-heating DSC scans are reported for PBTEHC and PBTHDDT. Gel permeation chromatography (GPC) analysis was performed using a Polymer Lab Model 120 gel

Table 1. Molecular Weight, Thermal, and Photophysical Properties of Polybenzobisthiazoles

polymer	M_n (kDa)	M_w (kDa)	PDI	T_m/T_c (°C)	$\lambda_{max}{}^b$ (nm)	$\lambda_{max}{}^c$ (nm)	E_g^{opt} (eV)	$PL_{max}{}^b$ (nm)	$PL_{max}{}^c$ (nm)
PBTOT-1	8.06	15.4	1.91	290/265	490	540	1.97	573	684
PBTOT-2	366.5	722.0	1.97	367/356	537	551	1.94	633	689
PBTEHC	6.8	11.4	1.68	348	460	471	2.18	535	572
PBTHDDT	19.94	56.7	2.84	364	512	508	2.13	582	583
PBTEHS	7.82	19.2	2.46	—[a]	550	549	1.92	598	660
PBTPDT	9.87	13.9	1.41	—[a]	542	544	1.96	629	636
PBTDTP-1	10.3	32.1	3.12	—[a]	563	560	1.85	600	—[d]
PBTDTP-2	52.4	147.6	2.82	—[a]	574	562	1.83	650	—[d]

[a] No thermal transition was observed up to 390 °C. [b] In $(1-3) \times 10^{-6}$ M solution. [c] Thin film. [d] PL emission was not observed.

permeation chromatograph (DRI/high sensitivity refractive index detector and PL-BV400HT viscometer) against polystyrene standards in chlorobenzene at 60 °C. X-ray diffraction (XRD) data were collected from a Bruker-AXS D8 Focus diffractometer with Cu Kα beam (40 kV, 40 mA) in theta−2-theta scans (0.02 Å step size, 1 s/step). Polymer thin films for XRD were prepared by drop-casting from a concentrated solution (15−20 mg/mL) in 1,2-dichlorobenzene onto a glass slide followed by annealing for 5 min at 180 °C and drying on a vacuum oven (60 °C) for 4 h. Cyclic voltammetry was done on an EG&G Princeton Applied Research potentiostat/galvanostat (Model 273A). Data were analyzed by using a Model 270 electrochemical analysis system software on a PC computer. A three-electrode cell was used, using platinum wire electrodes as both counter and working electrodes. Silver/silver ion (Ag in 0.1 M $AgNO_3$ solution, Bioanalytical System, Inc.) was used as a reference electrode. An electrolyte solution of 0.1 M $TBAPF_6$ in acetonitrile was used in all experiments. Using the internal ferrocenium/ferrocene (Fc^+/Fc) standard, the redox potential values obtained in reference to a Ag/Ag^+ electrode were converted to the saturated calomel electrode (SCE) scale.[28b] A thin film of each polymer semiconductor was coated onto a platinum electrode from a concentrated solution in chloroform or 1,2-dichlorobenzene and dried in vacuum for 2 h. All solutions were purged with N_2 for 20 min before each experiment. UV−vis absorption spectra were collected on a Perkin-Elmer model Lambda 900 UV/vis/near-IR spectrophotometer. The photoluminescence (PL) emission spectra were obtained with a Photon Technology International (PTI) Inc. Model QM2001-4 spectrofluorimeter.

2.3. Fabrication and Characterization of Field-Effect Transistors. Organic field-effect transistors (OFETs) were fabricated in bottom-contact and bottom-gate geometry. Heavily n-doped silicon with a 200−300 nm thermally grown oxide acted as a gate electrode with a dielectric layer and the substrate. Gold source and drain electrodes (∼40 nm) with a thin chromium layer (∼2 nm) were patterned on the substrate by photolithography and lift-off processes. The width (W) and length (L) of the transistor channel are 800−1000 μm and 20−100 μm, respectively. The SiO_2 surface was treated with octyltrichlorosilane (OTS8). Polymer thin films were deposited onto the substrate from solutions (8 mg/mL) in hot 1,2-dichlorobenzene or 1,2,4-trichlorobenzene. The films were annealed at 200 °C for 10−30 min under inert conditions. Initial electrical characteristics were measured using an HP4145B semiconductor parameter analyzer in a nitrogen atmosphere. OFETs were then taken out of inert conditions and stored and tested in ambient dark lab conditions without any control of humidity. A Keithley 4200SCS was used for testing of the devices in air. The mobility was calculated from the saturation region.

2.4. Fabrication and Characterization of Photovoltaic Cells. Each polymer solution was prepared by adding 1 mL of 1,2-dichlorobenzene into a 5 mL vial containing 9 mg of the polymer sample. The sample was stirred until it completely dissolved, and the solution was filtered through a 0.45 μm GHP filter. $PC_{71}BM$ solution was prepared by dissolving 120 mg of $PC_{71}BM$ (ADS, Quebec, Canada) in 2 mL of 1,2-dichlorobenzene at room temperature by stirring in a glovebox for 2 h. The solution was stored in the glovebox for use after passing it through a 0.2 μm PTFE filter. The blend solution of polymer:$PC_{71}BM$ with a composition of 1:2 (w:w) was prepared by mixing 0.2 mL of the 9 mg/mL polymer solution with 0.06 mL of the 60 mg/mL $PC_{71}BM$ solution and stirred for 10 min. For mixed solvent, a small amount of 1,8-diiodooctane (DIO) or 1,8-octanedithiol (ODT) (ODCB:DIO/ODT = 100:2.5 v/v) was added to the polymer/$PC_{71}BM$ blend before stirring. Solar cells were fabricated by first spin-coating a PEDOT:PSS buffer layer on top of ITO-coated glass substrates (10 Ω/□, Shanghai B. Tree Tech. Consult Co., Ltd., Shanghai, China) at 3000 rpm for 40 s and annealed at 150 °C for 10 min under vacuum. The substrates were transferred to a glovebox for deposition of the active layer. The active layer was spin-coated on top of PEDOT:PSS layer from the polymer:$PC_{71}BM$ blend solution at room temperature. The spin-coating speed and time were 800 rpm and 20 s, respectively. The film processed without an additive was dried in a covered Petri dish for 80 min and then annealed on a hot plate at temperature of 180 °C for 10 min, whereas the film processed with an additive was dried in vacuum at room temperature. The devices were characterized under 100 mW/cm^2 AM 1.5 sunlight. The light intensity was calibrated by a Si photodiode (which was calibrated at the National Renewable Energy Laboratory (NREL). All the characterization steps were carried out under ambient laboratory air. The active area of the solar cells was 9 mm^2. The absorption spectra of polymer/fullerene BHJ films were directly measured on the solar cell devices.

3. RESULTS AND DISCUSSION

3.1. Synthesis and Characterization. The synthesis of benzobisthiazole-based copolymers and the starting comonomers are outlined in Scheme 1. Comonomer 2,6-bis(5-bromo-3-dodecylthiophen-2-yl)benzo[1,2-*d*;4,5-*d*′]bisthiazole (**1**) was prepared according to our previously reported method.[17] Stannylation of 2,6-bis(5-trimethyltin-3-dodecylthiophen-2-yl)benzo-[1,2-*d*;4,5-*d*′]bisthiazole (**2**) was obtained in high yield using *n*-butyllithium and trimethyltin chloride. Good solubility and high molecular weight of the benzobisthiazole-based copolymers were achieved by incorporating dodecyl side chains on the benzobisthiazole monomer **1** and **2** as well as the use of sufficiently long alkyl side chains on the donor comonomers. Copolymerization of monomer **1** or **2** with various donor comonomers was carried out by Stille coupling reaction using $Pd_2(dba)_3$ and P(*o*-Tol)$_3$ as catalyst and ligand in chlorobenzene[3e] or by Suzuki coupling using $Pd(OAc)_2$ in toluene (Scheme 1). The copolymers were purified by Soxhlet extraction with methanol and hexane and were obtained in high yields (60−92%). Gel-permeation chromatography (GPC) measurements in chlorobenzene

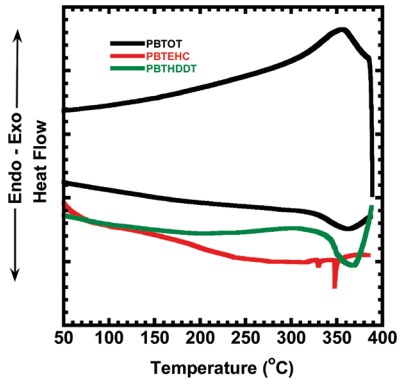

Figure 1. DSC scans of PBTOT, PBTEHC, and PBTHDDT at a heating/cooling rate of 10 °C/min in nitrogen.

solution, relative to polystyrene standards, showed moderate to high number-average molecular weight (M_n) that range from 6.8 kDa in PBTEHC to 366.5 kDa in PBTOT-2. The polydispersity index (PDI) varied from 1.41 to 3.12 (Table 1). Two fractions of PBTOT and PBTDTP were isolated based on the molecular weight as shown in Table 1. All eight copolymer samples were readily soluble in various organic solvents (chloroform, chlorobenzene, 1,2-dichlorobenzene, and 1,2,4-trichlorobenzene) to varying degree.

The thermal transition properties of the polybenzobisthiazoles were investigated by differential scanning calorimetry (DSC). Second-heating scan of PBTOT and first-heating scans of PBTEHC and PBTHDDT are shown in Figure 1, and the melting transition temperature (T_m) and the corresponding recrystallization temperature (T_c) are summarized in Table 1. A lower melting transition was observed in PBTOT-1 (T_m = 290 °C and T_c = 265 °C) compared to the higher molecular weight-fraction PBTOT-2 (T_m = 367 °C and T_c = 356 °C). High melting transitions were observed in PBTEHC (T_m = 348 °C) and PBTHDDT (T_m = 364 °C) despite their long and branched side alkyl chains. The observed melting transition in these polybenzobisthiazoles are significantly higher than the melting transition temperatures in poly(3-alkylthiophenes) (200−205 °C).[6b] Thermal transitions were not observed in the DSC scans of PBTEHS, PBTPDT, and PBTDTP up to 390 °C, suggesting that these polymers are thermally robust.

3.2. Photophysics. The photophysics of the new polybenzobisthiazoles was investigated by absorption and photoluminescence (PL) emission spectroscopy of the polymers in dilute solution and as thin films. Figure 2a shows the absorption spectra of the benzobisthiazole copolymers in dilute 1,2-dichlorobenzene solutions ((1−3) × 10^{-6} M). The absorption maxima (λ_{max}) of the six copolymers are summarized in Table 1. In solution, the polymers show one absorption band in the 330−650 nm range that can be assigned to the intramolecular charge transfer (ICT) band.[2a] A significant red-shift in the absorption maximum is observed as the donor comonomer is varied from carbazole to dithienopyrrole, indicative of increasing ICT strength with increasing donor strength.[2a]

The absorption spectra of the benzobisthiazole copolymers as thin films are shown in Figure 2b. The corresponding λ_{max} and optical band gap (E_g^{opt}) are summarized in Table 1. The thin film absorption spectra of the PBTs show some vibronic structure. All of the six PBTs show one absorption band in the range of 470−600 nm which can also be assigned to the ICT band.[2a] The

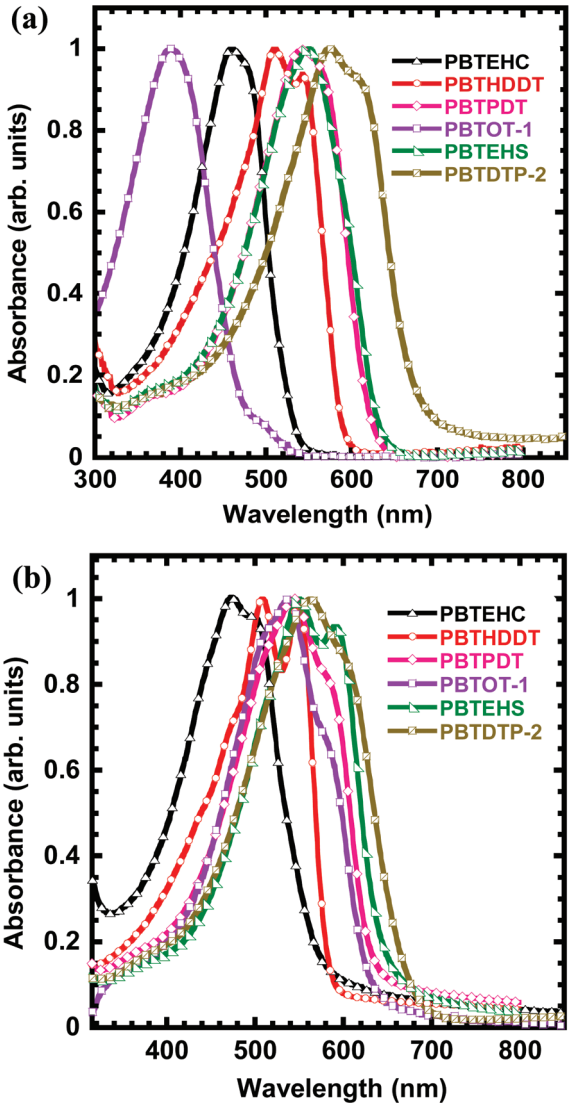

Figure 2. Optical absorption spectra of benzobisthiazole copolymers: (a) in dilute ((1−3) × 10^{-6} M) 1,2-dichlorobenzene solutions and (b) as thin films.

λ_{max} varies from 471 nm in PBTEHC to 562 nm in PBTDTP-2. A slight red-shift in the λ_{max} (551 nm) and an enhanced shoulder at 600 nm were observed in the higher molecular weight fraction PBTOT-2 compared to the λ_{max} of PBTOT-1 (540 nm), an indication of the strong interchain interactions in the solid state. In contrast, PBTDTP-1 and PBTDTP-2 showed identical absorption spectra, suggesting no significant difference in the molecular packing between the two fractions. The optical band gap (E_g^{opt}) of the PBTs varies from 2.18 eV in PBTEHC and 1.92 eV in PBTEHS to 1.83 eV in PBTDTP-2 (Table 1). As expected, the absorption maximum and the band gap of the PBTs are red-shifted and reduced, respectively, with increase in the ICT as the donor comonomer is varied. All of the six copolymers showed an enhanced absorption shoulder on the lower-energy side as thin films compared to the absorption in solution, an indication of improved intermolecular interactions and long-range order in the solid state. The tunable optical bands and relatively small optical band gaps of the PBTs suggest that they can also be used as light harvesting materials in solar cells.

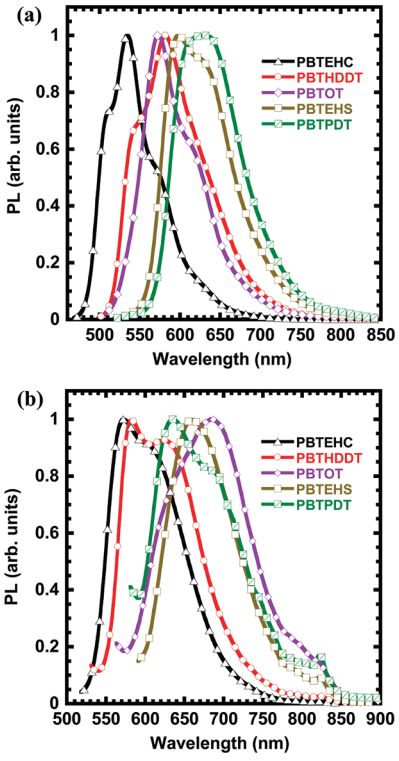

Figure 3. PL emission spectra of benzobisthiazole copolymers: (a) in dilute 1,2-dichlorobenzene solutions and (b) as thin films.

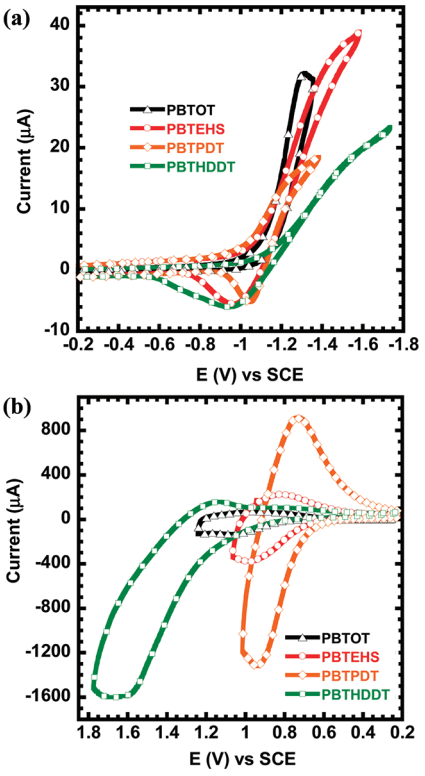

Figure 4. Cyclic voltammograms of polybenzobisthiazoles at a scan rate of 30−50 mV/s: (a) reduction waves and (b) oxidation waves.

Table 2. Electrochemical Properties of Polybenzobisthiazoles

polymer	E_{ox}^{onset} (V)	E_{red}^{onset} (V)	IP (eV)	EA (eV)	E_g^{el} (eV)
PBTOT-1	0.8	−1.1	5.2	3.30	1.90
PBTEHC	1.15	−1.10	5.55	3.30	2.25
PBTHDDT	1.31	−1.07	5.71	3.33	2.37
PBTEHS	0.69	−1.11	5.09	3.29	1.80
PBTPDT	0.73	−1.04	5.13	3.36	1.77
PBTDTP-2	0.39	−1.1	4.79	3.30	1.49

The PL emission spectra of the PBTs in dilute 1,2-dichlorobenzene solution and as thin films are shown in Figure 3. The PL emission maximum in solution and thin film are summarized in Table 2. As expected, a significant red-shift in the PL emission spectra is observed with increasing donor strength of the donor comonomer. The PL emission spectra of the six PBTs in dilute solution have an emission maximum in the range of 535−633 nm. In the solid state, emission spectra ranging from orange to red with a PL emission maximum of 572−689 nm are observed. The broad featureless PL emission spectra of the polybenzobisthiazoles can be attributed to aggregates and excimer emission in the solid state.[22a,b]

3.3. Redox Properties and HOMO/LUMO Energy Levels. Cyclic voltammetry was used to estimate the highest occupied molecular orbital (HOMO) and the lowest unoccupied molecular orbital (LUMO) energy levels and the corresponding ionization potential (IP)/electron affinity (EA) of the polybenzobisthiazoles. Cyclic voltammograms (CVs) of the PBTs, exemplified by those of PBTOT, PBTEHS, PBTPDT, and PBTHDDT, are shown in Figure 4. The copolymers showed quasi-reversible or irreversible reduction waves with onset reduction potentials of −1.1 to −1.04 V (vs SCE) (Figure 4a and Figure S1a). The estimated EA values or LUMO energy levels (EA = E_{red}^{onset} + 4.4 eV)[28] of all the PBTs were in the range 3.30−3.36 eV (Table 2). All of the six PBTs essentially have an identical LUMO energy level of −3.3 eV, which is not surprising given the constant benzobisthiazole acceptor moiety among all the copolymers. The present PBTs have a slightly lower-lying LUMO level compared to previously reported polybenzobisthiazoles (LUMO ∼ −2.4 to −3.0 eV)[23] and benzobisthiazole small-molecules (LUMO ∼ −2.7 to −3.4 eV).[26]

The observed oxidation CVs in Figure 4b and Figure S1b show quasi-reversible oxidation waves for all the PBTs except PBTHDDT, which has an irreversible oxidation wave. As expected, the oxidation potentials gradually become less positive with increasing strength of the donor comonomer. The onset oxidation potential (E_{ox}^{onset}) varied from 0.39 V in PBTDTP-2 to 1.31 V (vs SCE) in PBTHDDT (Table 2). The estimated IP values (IP = E_{ox}^{onset} + 4.4 eV)[28] thus varied from 4.79 eV in PBTDTP-2 to 5.71 eV in PBTHDDT (Table 2). The trends in the measured HOMO/LUMO energy levels of the PBTs and the relative donor strength of the comonomer are illustrated in Figure 5. These results clearly show that the HOMO energy level can be varied by up to 0.92 eV by varying the donor comonomer incorporated into the PBTs. The HOMO energy level of the new PBTs is lower by 0.19−0.81 eV compared to the poly(3-alkylthiophenes) (−4.9 eV), except in PBTDTP (−4.79 eV) containing the strong dithienopyrrole moiety, which significantly raises the HOMO energy level. The low-lying HOMO energy level in these benzobisthiazole copolymers suggests that they are oxidatively stable hole transporting materials.[11−18] In addition, low-lying HOMO energy levels are desired in bulk heterojunction

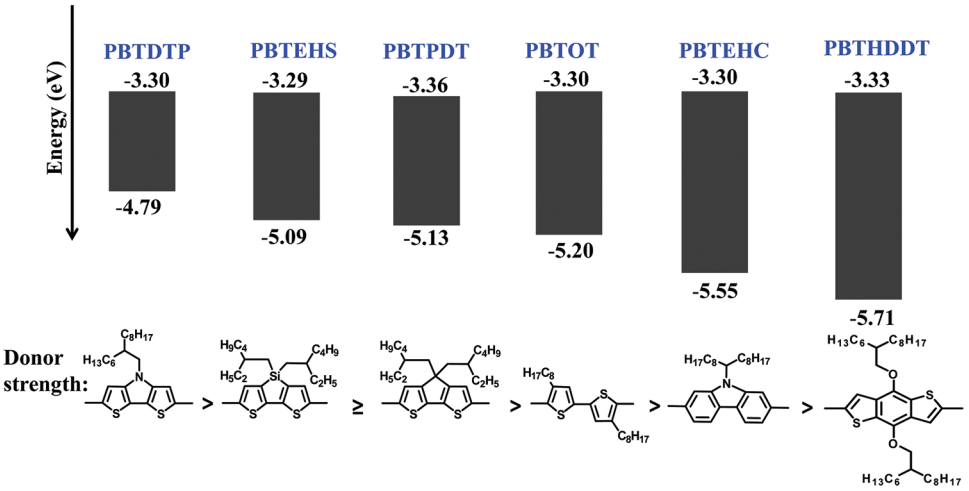

Figure 5. Graphic illustration of the HOMO/LUMO energy levels of polybenzobisthiazoles.

(BHJ) solar cells as an approach to maximize the open-circuit voltage (V_{oc}), which is known to be related to the difference in the donor polymer HOMO and the acceptor (fullerene) LUMO energy levels. The electrochemical band gap (E_g^{el}) of the PBTs varied from 1.49 eV in PBTDTP to 1.77 eV in PBTPDT and to 2.37 eV in PBTHDDT (Table 2). The E_g^{el} values differ from the E_g^{opt} values (Table 1) by about 70−340 meV, which is due in part to the binding energy of excitons in these organic semiconductors.[29]

3.4. Morphology and Molecular Packing. To investigate the solid-state morphology and supramolecular organization of the PBTs, we performed X-ray diffraction (XRD) analysis on thin films drop-casted from 1,2-dichlorobenzene solution onto a glass substrate. The thin films were annealed at 180 °C for 5 min and then dried in a vacuum oven (60 °C) for 4 h. The XRD spectra of the six copolymer films are shown in Figure 6, and the reflection peaks and the corresponding *d*-spacings are summarized in Table 3. The X-ray diffraction pattern of the octyl-substituted copolymer (PBTOT-2) films showed three diffraction peaks at $2\theta = 5.66°$, 11.1°, and 16.4°. The strong diffraction peaks and the high-order peak (300) suggest a high degree of crystallinity in the PBTOT-2 films. In contrast, the XRD pattern of the lower molecular weight PBTOT-1 film showed only two diffraction peaks at $2\theta = 5.58°$ and 11.1°. The diffraction peak at 5.66° corresponds to an interlayer lamellar d_{100}-spacing of 15.6 Å. The observed interlayer d_{100}-spacing in PBTOT is much smaller than that in poly(3-octylthiophene) (P3OT) (20.1 Å)[6b] and that in poly(3-hexylthiophene) (P3HT) (16.3 Å).[6b] The X-ray diffraction patterns of both PBTOT-1 and PBTOT-2 did not show any reflection peak that correspond to the π-stacking direction.

The X-ray diffraction patterns of similarly prepared films of PBTEHC, PBTHDDT, PBTEHS, PBTPDT, PBTDTP-1, and PBTDTP-2 showed strong diffraction peaks in the range of $2\theta = 4.16°-4.82°$, corresponding to a lamellar ordering with *d*-spacings of 18.3-21.2 Å and can be assigned to the (100) reflection. The larger *d*-spacing of these six copolymers compared to PBTOT is due to the longer dodecyl side chains. However, these interchain d_{100}-spacings of the PBTs are still significantly smaller than those of poly(3-dodecylthiophene) (P3DDT) (27.19 Å)[6b] and poly(3-decylthiophene) (P3DT) (23.88 Å).[6b] The observed interlayer distance is about 22−32% smaller than in the corresponding poly(3-alkylthiophene), which

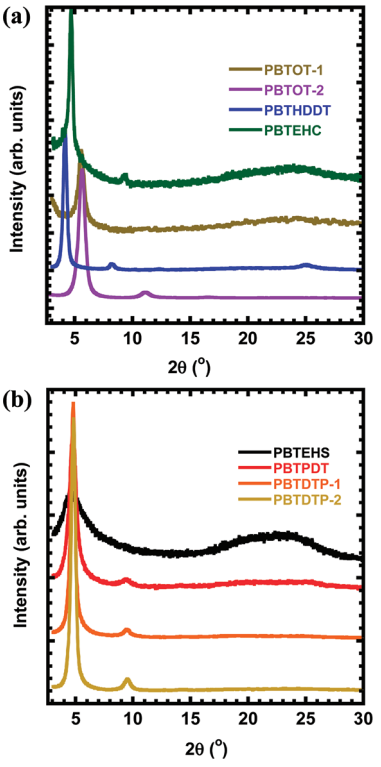

Figure 6. XRD spectra of benzobisthiazole copolymer thin films.

suggests that the alkyl chains in the polybenzobisthiazoles strongly interdigitate. These results are not surprising; the organization of the side chains of several alkyl-chain-substituted polymers is known to be via interdigitation due to the free space enabled by a low grafting density of side chains.[11−13] Second-order diffraction peaks in all of the six copolymers, except PBTEHS, are observed in the range of $2\theta = 8.18°-9.5°$. The relatively broad diffraction peaks in PBTEHC, PBTEHS PBTPDT, PBTDTP-1, and PBTDTP-2 and the sharp diffraction peak in PBTHDDT in the range of $2\theta = 23.5°-25.2°$ correspond to *d*-spacings of 3.53−3.78 Å and can be assigned to the reflection due to π-stacking (Figure S2). The observed π-stacking distances are significantly smaller than the measured π-stacking distance in

Table 3. XRD Reflections and *d*-Spacings of Polybenzobisthiazoles

	2θ (deg) (*d*-spacing (Å)) for reflections			
polymer	(100)	(200)	(300)	(d_π)
PBTOT-1	5.58 (15.8)	11.1		
PBTOT-2	5.66 (15.6)	11.1	16.4	
PBTEHC	4.70 (18.8)	9.48		24.0 (3.70)
PBTHDDT	4.16 (21.2)	8.18		25.2 (3.53)
PBTEHS	4.60 (19.2)			23.5 (3.78)
PBTPDT	4.80 (18.4)	9.42		23.5 (3.78)
PBTDTP-1	4.80 (18.4)	9.40		24.4 (3.64)
PBTDTP-2	4.82 (18.3)	9.5		24.4 (3.64)

P3DDT (3.95 Å) but are smaller than or comparable to that of P3HT (3.79 Å).[6b] It is remarkable that the observed π-stacking distances are significantly smaller despite the bulky branched alkyl chains in the donor comonomers of the PBTs. Thus, it is reasonable to predict that the π-stacking distance in polybenzobisthiazoles with linear alkyl chains such as PBTOT could be even smaller than 3.5 Å.

3.5. Field-Effect Transistors. The charge transport properties of the polybenzobisthiazoles were investigated by fabricating and testing field-effect transistors using a bottom-contact and bottom-gate geometry.[14a,b] Clear current modulation and saturation were seen in the output and transfer characteristics of the OFETs based on the series of PBTs as exemplified by those of PBTDTP-2 shown in Figure 7. The carrier mobility (μ_h), on/off current ratio, and the threshold voltage (V_t) of OFETs based on the PBTs are listed in Table 4. A hole mobility ranging from 1.8×10^{-4} cm^2/(V s) in PBTDTP-1 to 0.011 cm^2/(V s) in PBTEHC was observed with on/off current ratio in the range of 10^3-10^6 and a threshold voltage in the -5.2 to -28.6 V range. All of the polybenzobisthiazoles thus exhibit good p-type charge transport properties with small variations in the carrier mobility and on/off current ratio as the electron-donating unit in the backbone was varied.

Significant contact resistance was observed from the output characteristics of PBTHDDT and PBTEHC devices (Figures S3 and S4) as indicated by the superlinearity of current in the linear region, i.e., low source-drain bias under high source-gate bias. This can be explained by the high IPs of both polymers (5.55−5.71 eV), which lead to a large charge injection barrier from gold source-drain electrodes with a work function of ~5.1 eV. Nevertheless, the highly crystalline nature of films of the PBTs, as revealed by their XRD patterns, facilitated good charge transport with hole mobility as high as 0.006−0.011 cm^2/(V s).

It is not surprising that PBTEHS and PBTPDT, whose molecular structures differ only by one atom, silicon atom versus a carbon atom, respectively, at the five-membered ring on the electron-donating moiety, had very similar charge-transport properties with a similar charge-carrier mobility of $(6-8) \times 10^{-4}$ cm^2/(V s) and a threshold voltage (−22, −23 V). As shown in Tables 1 and 2, these two polymers also have similar molecular weight and HOMO/LUMO energy levels and optical band gap. Given that both molecular structure and morphology govern the charge transport properties of polymer semiconductors, the effect of a small change in molecular structure is insignificant for overall charge transport properties of these two members of the PBTs.

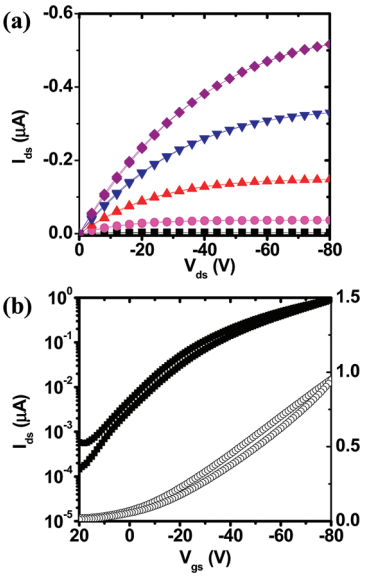

Figure 7. Output (a) and transfer (b) characteristics of a PBTDTP-2 OFET.

Table 4. Field-Effect Charge Transport Properties of Polybenzobisthiazoles

polymer	μ_h^{avg} (cm^2/(V s))	μ_h^{max} (cm^2/(V s))	I_{on}/I_{off}	V_t (V)
PBTOT-1	0.002	0.002	10^5	−19.0
PBTOT-2	0.009	0.01	10^6	−5.2
PBTDTP-1	1.8×10^{-4}	2.2×10^{-4}	10^4	−28.6
PBTDTP-2	5.3×10^{-4}	5.5×10^{-4}	10^3	−3.7
PBTEHC	0.0097	0.011	10^5	−15.3
PBTEHS	6.4×10^{-4}	7.2×10^{-4}	10^4	−22.8
PBTHDDT	0.0063	0.0093	10^4	−20.9
PBTPDT	6.8×10^{-4}	8.5×10^{-4}	10^5	−22.1

Field-effect transistors were fabricated from both the high and low molecular weight fractions of PBTOT and PBTDTP to assess the effect of molecular weight on charge transport of this class of polymer semiconductors. The charge-carrier mobility in the PBTs seems to increase by a factor of 3−5 as the molecular weight increases. Enhancement of charge-carrier mobility with increasing molecular weight has been observed in other conjugated polymers including P3HT.[9] The higher charge-carrier mobility in the higher molecular weight sample is explained by the reduced defects from chain ends and improved interchain interactions.

To investigate the stability/durability of OFETs fabricated from the polybenzobisthiazoles, we measured the performance (μ_h, $I_{on/off}$, V_t) of PBTOT-2 OFET as a function of time in ambient air conditions (Figure 8). The OFETs were initially tested in a nitrogen-filled drybox, brought out and tested in air, and then stored and periodically tested in ambient air conditions. Figure 8a−c shows that the carrier mobility, threshold voltage, and the on/off current ratio essentially remained the same for almost 2 years. A slight change in the initial carrier mobility measured in nitrogen (0.009 cm^2/(V s)) compared with the first measurement in air (0.007 cm^2/(V s)) was observed. The carrier mobility measured after 721 days was 0.006 cm^2/(V s). Similarly, a slight variation in the initial threshold voltage measured in

dx.doi.org/10.1021/ma201128x |*Macromolecules* 2011, 44, 7207–7219

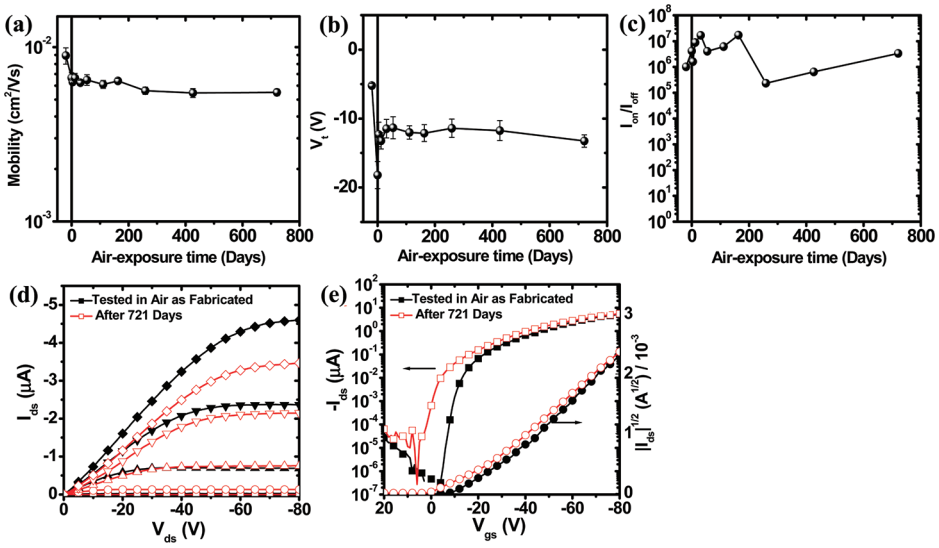

Figure 8. Performance of PBTOT-2 OFETs as a function of air-exposure time (a) mobility of holes, (b) threshold voltage, and (c) on/off current ratio. An overlay of the (d) output and (e) transfer characteristics of PBTOT-2 devices tested for almost 2 years. Devices first measured in N_2-filled drybox were brought out and stored and periodically tested in ambient conditions.

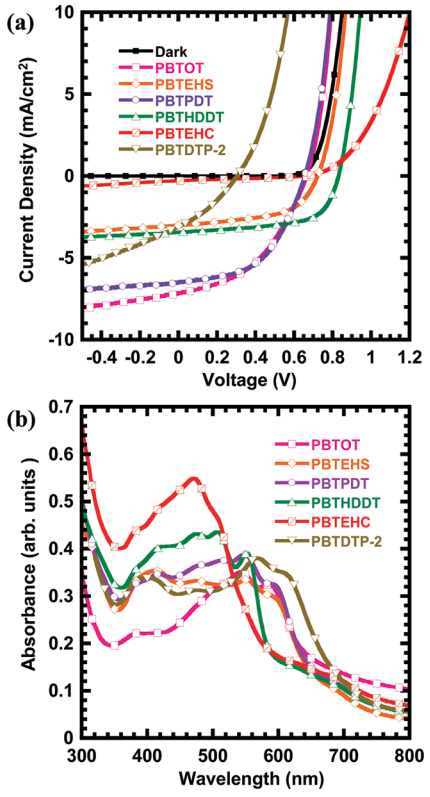

Figure 9. (a) Current density−voltage curves of PBT:$PC_{71}BM$ (1:2) devices under 100 mW/cm^2 AM 1.5 solar irradiation and in the dark. (b) Optical absorption spectra of PBT: $PC_{71}BM$ (1:2) blend films on glass/ITO/PEDOT substrates.

nitrogen (−5 V) compared to the first measurement in air (−18 V) was observed, and after 4 days it stabilizes at −13 V for up to 721 days. Figure 8d,e shows slight changes in the transfer and output characteristics of days 1 and 721 measurements in air. The remarkable durability of the PBTOT FET devices is in part due to its low-lying HOMO level (∼−5.2 eV) and consequent resistance to unintentional oxidation in air and the high degree of crystallinity of the polymer films which enables resistance to oxygen and moisture diffusion.

Table 5. Photovoltaic Properties of Polybenzobisthiazoles BHJ Solar Cells

active layer	J_{sc} (mA/cm^2)	V_{oc} (V)	FF	η_{avg} (η_{max}) (%)
PBTOT-1:$PC_{71}BM$ (1:1)[a]	7.08	0.66	0.45	2.07 (2.1)
PBTEHS:$PC_{71}BM$ (1:2)[a]	3.01	0.73	0.55	1.21 (1.24)
PBTPDT:$PC_{71}BM$ (1:2)[a]	6.58	0.65	0.51	2.16 (2.20)
PBTHDDT:$PC_{71}BM$ (1:2)[a]	3.42	0.81	0.63	1.76 (1.79)
PBTEHC:$PC_{71}BM$ (1:2)[a]	0.29	0.65	0.32	0.06
PBTDTP-1:$PC_{71}BM$ (1:2)[a]	1.30	0.36	0.19	0.09 (0.10)
PBTDTP-2:$PC_{71}BM$ (1:2)[a]	3.06	0.31	0.32	0.30 (0.31)
PBTOT-1:$PC_{71}BM$ (1:1)[b]	6.55	0.615	0.41	1.67 (1.7)
PBTEHS:$PC_{71}BM$ (1:2)[c]	5.98	0.62	0.55	2.02 (2.03)
PBTPDT:$PC_{71}BM$ (1:2)[c]	7.96	0.55	0.38	1.66 (1.68)
PBTHDDT:$PC_{71}BM$ (1:2)[c]	7.22	0.63	0.64	2.94 (3.00)
PBTEHC:$PC_{71}BM$ (1:2)[c]	1.17	0.61	0.54	0.38 (0.39)

[a] No processing additive was used. [b] 1,8-Octanedithiol (ODT) was used as the processing additive with ODCB (ODCB:ODT = 100:2.5, v/v). [c] 1,8-Diiodooctane (DIO) was used as the processing additive with ODCB (ODCB:DIO = 100:2.5, v/v).

3.6. Solar Cells. We fabricated and characterized bulk heterojunction (BHJ) solar cells based on binary blends of each PBTs with $PC_{71}BM$, resulting in photodiodes with the structure ITO/PEDOT:PSS/blend/LiF/Al. The active layers (PBT:$PC_{71}BM$ blend) were spin-coated from 1,2-dichlorobenzene solution with a thickness in the range 60−80 nm. The current density−voltage characteristics of the PBT:$PC_{71}BM$ (1:2) blend solar cell under dark and under 100 mW/cm^2 AM1.5 solar illumination are shown in Figure 9a. The photovoltaic parameters, including the short-circuit current density (J_{sc}), the open-circuit voltage (V_{oc}), the fill factor (FF), and the average (η_{avg}) and maximum (η_{max}) power conversion efficiency are summarized in Table 5.

The V_{oc} of the solar cells varies from 0.81 V in PBTHDDT:$PC_{71}BM$ to 0.31 V in PBTDTP:$PC_{71}BM$. This variation in V_{oc} can generally be understood from the observed difference in their HOMO energy level, which ranges from −5.71 eV in PBTHDDT to −4.79 eV in PBTDTP. However, the change in the V_{oc} from 0.66 V in PBTOT-1:$PC_{71}BM$ to 0.73 V in PBTEHS:$PC_{71}BM$ to 0.65 V in PBTEHC and PBTPDT cannot be easily explained solely by the differences in the HOMO energy levels, which ranged from −5.2 eV in PBTOT-1 to −5.10 eV in PBTEHS and PBTPDT to −5.55 eV in PBTEHC. We assume that the observed variation in the V_{oc} is also due to other factors such as the blend morphology which has been reported to influence the V_{oc}.[30] Initial BHJ solar cells based on PBTOT-1:$PC_{71}BM$ and PBTPDT:$PC_{71}BM$ systems gave the highest power conversion efficiency of 2.1−2.2% with high J_{sc} (6.58−7.08 mA/cm^2), V_{oc} of 0.65−0.66 V and FF of 0.45−0.51. The similar V_{oc} in PBTOT-1:$PC_{71}BM$ and PBTPDT:$PC_{71}BM$ systems can be understood from their similar HOMO energy levels (−5.1/-5.2 eV). The poor FF (0.45) in PBTOT-1:$PC_{71}BM$ compared to PBTPDT:$PC_{71}BM$ (FF = 0.51) cannot be explained on the basis of charge transport since a higher carrier mobility was found in PBTOT-1 (0.002 cm^2/(V s)) than in PBTPDT (6.8×10^{-4} cm^2/(V s)). Other factors that could have contributed to the difference in the FF include high series resistance due to unfavorable morphology and high rate of charge recombination. The photovoltaic efficiency in PBTEHS devices (1.24% PCE) is significantly lower than in PBTPDT despite their similar molecular structures and essentially identical HOMO energy levels (−5.1/−5.13 eV), similar absorption bands (Figure 9b), and similar carrier mobilities. This difference in the performance is likely a result of variation in the blend morphology. Interestingly, the rather high V_{oc} (0.81 V) in the PBTHDDT:$PC_{71}BM$ blend system does not translate to a higher solar cell efficiency (1.79%) primarily because of the poor photocurrent. On the other hand, the narrow absorption band in PBTEHC:$PC_{71}BM$ system (Figure 9b) and the high-lying HOMO level of PBTDTP (−4.79 eV) contributed to their observed poor power conversion efficiency (0.06−0.31%).

Optimization of selected polybenzobisthiazole:$PC_{71}BM$ devices was carried out in effort to improve the power conversion efficiency by adding a processing additive, 1,8-diiodooctane (DIO) or 1,8-octanedithiol (ODT), into the main solvent 1, 2-dichlorobenzene (ODCB:DIO 100:2.5 v/v) used in the film deposition. The resulting blend films were dried in vacuum (about 10^{-3} Torr) for 30 min without any thermal annealing. Such processing additives are thought to improve the two-phase morphology in BHJ polymer solar cells.[31] The current density−voltage characteristics of the PBT:$PC_{71}BM$ (1:2) blend solar cells fabricated by using a processing additive and the corresponding optical absorption spectra are shown in Figure 10. The photovoltaic properties (J_{sc}, V_{oc}, FF, and η) of these BHJ solar cells are also summarized in Table 5. In general, a decrease in the V_{oc} is observed when using a processing additive while an increase in J_{sc} is observed except in the PBTOT-1:$PC_{71}BM$ and PBTPDT:$PC_{71}BM$ systems. BHJ solar cells based on PBTHDDT:$PC_{71}BM$ gave the highest power conversion efficiency of 3.0% with a J_{sc} of 7.22 mA/cm^2, a V_{oc} of 0.63 V, and a FF of 0.64 when using DIO as the processing additive. The enhancement in the PCE of PBTHDDT:$PC_{71}BM$ devices is largely due to an increase in the J_{sc} even though the V_{oc} significantly decreased from 0.81 to 0.63 V while the FF was unchanged. These results suggest that further device optimization including

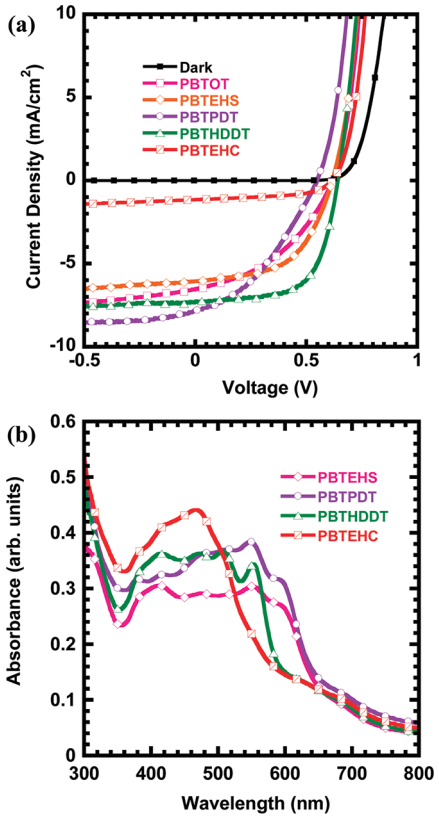

Figure 10. (a) Current density−voltage curves of PBT:$PC_{71}BM$ (1:2) devices under 100 mW/cm^2 AM 1.5 solar irradiation and in the dark. (b) Optical absorption spectra of PBT:$PC_{71}BM$ (1:2) blend films on glass/ITO/PEDOT substrates. All blend films processed from a mixed solvent of 1,2-dichlorobenzene:1,8-diiodooctane (100:2.5, v/v).

blend composition, active layer film thickness and annealing conditions could further improve the efficiency of PBTHDDT devices. A significant decrease in the power conversion efficiency in PBTOT-1:$PC_{71}BM$ (1.7%) and PBTPDT:$PC_{71}BM$ (1.68%) BHJ solar cells as a result of a decrease in the FF and the V_{oc} was observed when using a processing additive. Thin films of PBTPDT:$PC_{71}BM$ blend show nearly identical absorption characteristics with or without using a processing additive, suggesting that the difference in solar cell performance does not come from the light harvesting.

4. CONCLUSIONS

A series of six new donor−acceptor copolymer semiconductors based on benzobisthiazole and various donor moieties have been synthesized by Stille or Suzuki coupling polymerization. The optical absorption of the new polybenzobisthiazoles (PBTs) was tuned by varying the strength of the donor segment, resulting in an optical band gap in the range 1.83−2.18 eV. All six PBTs have a similar electrochemistry-derived LUMO energy level (∼−3.3 eV), whereas the HOMO energy level could be varied in the range −4.79 to −5.71 eV. X-ray diffraction of solution-casted films of PBTs showed highly crystalline structures with an interlayer d_{100}-spacing of 15.6 Å in PBTOT to 18.3 Å in PBTDTP and 21.2 Å in PBTHDDT, which are shorter by 22−32% compared to the interlayer d_{100}-spacing in poly(3-octylthiophene) (P3OT) (20.1 Å) and poly(3-dodecylthiophenes) (P3DDT) (27.19 Å). X-ray diffraction also showed that the PBTs exhibit a

short π-stacking distance (3.53−3.78 Å). As semiconductors in p-channel field-effect transistors the PBTs have a carrier mobility as high as 0.011 $cm^2/(V\ s)$ and on/off current ratios of up to 10^6. The carrier mobility, threshold voltage, and on/off current ratio of the PBT transistors showed remarkable stability/durability in ambient air for almost 2 years. BHJ solar cells developed from the PBTs have a power conversion efficiency of up to 3.0%. These results show that the highly crystalline, thermally robust, and oxidatively stable polybenzobisthiazoles are promising semiconductors for field-effect transistors and solar cells.

■ ASSOCIATED CONTENT

Supporting Information. Cyclic voltammetry scans, XRD spectra, ^{1}H NMR spectra, and electrical characteristics of field-effect transistors. This material is available free of charge via the Internet at http://pubs.acs.org.

■ AUTHOR INFORMATION

Corresponding Author
*E-mail: jenekhe@u.washington.edu.

■ ACKNOWLEDGMENT

This report is based on research (excitonic solar cells) supported by the U.S. DOE, Basic Energy Sciences, Division of Materials Science, under Award DE-FG02-07ER46467. The synthesis and characterization of p-type polymer semiconductors was supported by the NSF (DMR 0805259 and DMR 0120967) and in part by Solvay S. A.

■ REFERENCES

(1) (a) Thompson, B. C.; Frechet, J. M. J. *Angew. Chem., Int. Ed.* **2008**, *47*, 58. (b) Cheng, Y.-J.; Yang, S.-H.; Hsu, C.-S. *Chem. Rev.* **2009**, *109*, 5868. (c) Boudreault, P.-L. T.; Najari, A.; Leclerc, M. *Chem. Mater.* **2011**, *23*, 456. (d) Kim, F. S.; Ren, G.; Jenekhe, S. A. *Chem. Mater.* **2011**, *23*, 682.

(2) (a) Jenekhe, S. A.; Lu, L.; Alam, M. M. *Macromolecules* **2001**, *34*, 7315. (b) Kroon, R.; Lenes, M.; Hummelen, J. C.; Blom, P. W.; de Boer, B. *Polym. Rev.* **2008**, *48*, 531. (c) Bull, T. A.; Pingree, L. S. C.; Jenekhe, S. A.; Ginger, D. S.; Luscombe, C. K. *ACS Nano* **2009**, *3*, 627. (d) Xin, H.; Guo, X.; Kim, F. S.; Ren, G.; Watson, M. D.; Jenekhe, S. A. *J. Mater. Chem.* **2009**, *19*, 5303.

(3) (a) Subramaniyan, S.; Xin, H.; Kim, F. S.; Shoaee, S.; Durrant, J. R.; Jenekhe, S. A. *Adv. Energy Mater.* **2011**, DOI: 10.1002/aenm.201100215. (b) Subramaniyan, S.; Xin, H.; Kim, F. S.; Jenekhe, S. A. *Macromolecules* **2011**, DOI: 10.1021/ ma-2011-01054a. (c) Wu, P.-T.; Bull, T.; Kim, F. S.; Luscombe, C. K.; Jenekhe, S. A. *Macromolecules* **2009**, *42*, 671. (d) Guo, X.; Xin, H.; Kim, F. S.; Liyanage, A. D. T.; Jenekhe, S. A.; Watson, M. D. *Macromolecules* **2011**, *44*, 269. (e) Zhu, Y.; Champion, R. D.; Jenekhe, S. A. *Macromolecules* **2006**, *39*, 8712. (f) Wu, P.-T.; Kim, F. S.; Champion, R. D.; Jenekhe, S. A. *Macromolecules* **2008**, *41*, 7021.

(4) (a) Liang, Y.; Xu, Z.; Xia, J.; Tsai, S.-T.; Wu, Y.; Li, G.; Ray, C.; Yu, L. *Adv. Mater.* **2010**, *22*, E135. (b) Blouin, N.; Michaud, A.; Gendron, D.; Wakim, S.; Blair, E.; Neagu-Plesu, R.; Belletête, M.; Durocher, G.; Tao, Y.; Leclerc, M. *J. Am. Chem. Soc.* **2008**, *130*, 732. (c) Park, S. H.; Roy, A.; Beaupré, S.; Cho, S.; Coates, N.; Moon, J. S.; Moses, D.; Leclerc, M.; Lee, K.; Heeger, A. J. *Nature Photonics* **2009**, *3*, 297. (d) He, Y.; Wang, X.; Zhang, J.; Li, Y. *Macromol. Rapid Commun.* **2009**, *30*, 45.

(5) (a) Steckler, T. T.; Zhang, Z.; Hwang, J.; Honeyager, R.; Ohira, S.; Zhang, X.-H.; Grant, A.; Ellinger, S.; Odom, S. A.; Sweat, D.; Tanner, D. B.; Rinzler, A. G.; Barlow, S.; Bredas, J.-L.; Kippelen, B.; Marder, S. R.; Reynolds, J. R. *J. Am. Chem. Soc.* **2009**, *131*, 2824. (b) Wienk, M. M.; Turbiez, M.; Gilot, J.; Janssen, R. A. J. *Adv. Mater.* **2008**, *20*, 2556. (c) Hou, J.; Park, M.-H.; Zhang, S.; Yao, Y.; Chen, L.-M.; Li, J.-H.; Yang, Y. *Macromolecules* **2009**, *41*, 6012.

(6) (a) McCullough, R. D.; Tristram-Nagle, S.; Williams, S. P.; Lowe, R. D.; Jayaraman, M. *J. Am. Chem. Soc.* **1993**, *115*, 4910. (b) Chen, T.-A.; Wu, X.; Rieke, R. D. *J. Am. Chem. Soc.* **1995**, *117*, 233.

(7) (a) Bao, Z.; Dobablapur, A.; Lovinger, A. J. *Appl. Phys. Lett.* **1996**, *69*, 4108. (b) Sirringhaus, H.; Tessler, N.; Friend, R. H. *Science* **1998**, *280*, 1741. (c) Babel, A.; Jenekhe, S. A. *J. Phys. Chem. B* **2003**, *107*, 1749.

(8) (a) Xin, H.; Kim, F. S.; Jenekhe, S. A. *J. Am. Chem. Soc.* **2008**, *130*, 5424. (b) Xin, H.; Kim, F. S.; Ren, G.; Jenekhe, S. A. *Chem. Mater.* **2008**, *20*, 6199.

(9) (a) Kline, R. J.; McGehee, M. D.; Kadnikova, E. N.; Liu, J.; Fréchet, J. M. J. *Adv. Mater.* **2003**, *15*, 1519. (b) Zen, A.; Saphiannikova, M.; Nehr, D.; Grenzer, J.; Grigorian, S.; Pietsch, U.; Asawapirom, U.; Janietz, S.; Scherf, U.; Lieberwirth, I.; Wegner, G. *Macromolecules* **2006**, *39*, 2162. (c) Zhang, R.; Li, B.; Iovu, M. C.; Jeffries-EL, M.; Sauvé, G.; Cooper, J.; Jia, S.; Tristram-Nagle, S.; Smilgies, D. M.; Lambeth, D. N.; McCullough, R. D.; Kowalewski, T. *J. Am. Chem. Soc.* **2006**, *128*, 3480.

(10) (a) Babel, A.; Jenekhe, S. A. *Synth. Met.* **2005**, *148*, 169. (b) Zen, A.; Saphiannikova, M.; Neher, D.; Asawapirom, U.; Scherf, U. *Chem. Mater.* **2005**, *17*, 781.

(11) (a) Ong, B. S.; Wu, Y.; Gardner, S. *J. Am. Chem. Soc.* **2004**, *126*, 3378. (b) Pan, H.; Wu, Y.; Li, Y.; Liu, P.; Ong, B. S.; Zhu, S.; Xu, G. *Adv. Funct. Mater.* **2007**, *17*, 3574.

(12) (a) McCulloch, I.; Heeney, M.; Bailey, C.; Genevicius, K.; Macdonald, I.; Shkunov, M.; Sparrowe, D.; Tierney, S.; Wagner, R.; Zhang, W.; Chabinyc, M. L.; Kline, R. J.; McGehee, M. D.; Toney, M. F. *Nature Mater.* **2006**, *5*, 328. (b) Li, Y.; Wu, Y.; Liu, P.; Birau, M.; Pan, H.; Ong, B. S. *Adv. Mater.* **2006**, *18*, 3029.

(13) (a) Pan, H.; Wu, Y.; Li, Y.; Ong, B. S.; Zhu, S.; Gu, X. *Adv. Funct. Mater.* **2007**, *17*, 3574. (b) Heeney, M.; Bailey, C.; Genevicius, K.; Shkunov, M.; Sparrowe, D.; Tierney, S.; McCulloch, I. *J. Am. Chem. Soc.* **2005**, *127*, 1078.

(14) (a) Guo, X.; Kim, F. S.; Jenekhe, S. A.; Watson, M. D. *J. Am. Chem. Soc.* **2009**, *131*, 7206. (b) Kim, F. S.; Guo, X.; Watson, M. D.; Jenekhe, S. A. *Adv. Mater.* **2010**, *22*, 478. (c) Nelson, T. L.; Young, T. M.; Liu, J.; Mishra, S. P.; Belot, J. A.; Balliet, C. L.; Javier, A. E.; Kowalewski, T.; McCullough, R. D. *Adv. Mater.* **2010**, *22*, 4617. (d) Tsao, H. N.; Cho, D.; Andreasen, J. W.; Rouhanipour, A.; Breiby, D. W.; Pisula, W.; Müllen, K. *Adv. Mater.* **2009**, *21*, 209.

(15) (a) Osaka, I.; Zhang, R.; Sauve, G.; Smilgies, D.-M.; Kowalewski, T.; McCullough, R. D. *J. Am. Chem. Soc.* **2009**, *131*, 2521. (b) Osaka, I.; Sauve, G.; Zhang, R.; Kowalewski, T.; McCullough, R. D. *Adv. Mater.* **2007**, *19*, 4160. (c) Narazo; Wudl, F. *Macromolecules* **2008**, *41*, 3169.

(16) (a) Kim, D. H.; Lee, B.-L.; Moon, H.; Kang, H. M.; Jeong, E. J.; Park, J.-L.; Han, K.-M.; Lee, S.; Yoo, W. B.; Koo, B. W.; Kim, Y.; Lee, W. H.; Cho, K.; Becerril, H. A.; Bao, Z. *J. Am. Chem. Soc.* **2009**, *131*, 6124. (b) Yang, C.; Cho, S.; Chiechi, R. C.; Walker, W.; Coates, N. E.; Daniel, M.; Heeger, A. J.; Wudl, F. *J. Am. Chem. Soc.* **2008**, *130*, 16524.

(17) Ahmed, E.; Kim, F. S.; Xin, H.; Jenekhe, S. A. *Macromolecules* **2009**, *42*, 6815.

(18) Osaka, I.; Takimiya, K.; McCullough, R. D. *Adv. Mater.* **2010**, *22*, 4993.

(19) Babel, A.; Jenekhe, S. A. *J. Am. Chem. Soc.* **2003**, *125*, 13656.

(20) Babel, A.; Jenekhe, S. A. *J. Phys. Chem. B* **2002**, *106*, 6129.

(21) (a) Wolfe, J. F.; Loo, B. H.; Arnold, F. E. *Macromolecules* **1981**, *14*, 915. (b) Choe, E. W.; Kim, S. N. *Macromolecules* **1981**, *14*, 920.

(22) (a) Jenekhe, S. A.; Osaheni, J. A. *Science* **1994**, *265*, 765. (b) Osaheni, J. A.; Jenekhe, S. A. *J. Am. Chem. Soc.* **1995**, *117*, 7389. (c) Roberts, M. F.; Jenekhe, S. A. *Chem. Mater.* **1993**, *5*, 1744. (d) Osaheni, J. A.; Jenekhe, S. A. *Chem. Mater.* **1995**, *7*, 672. (e) So, Y.-H.; Zaleski, J. M.; Murlick, C.; Ellaboudy, A. *Macromolecules* **1996**, *29*, 2783.

(23) (a) Osaheni, J. A.; Jenekhe, S. A. *Macromolecules* **1993**, *26*, 4726. (b) Alam, M. M.; Jenekhe, S. A. *Chem. Mater.* **2002**, *14*, 4775.

(24) (a) Jenekhe, S. A.; Osaheni, J. A.; Meth, J. S.; Vanherzeele, H. *Chem. Mater.* **1992**, *4*, 683. (b) Osaheni, J. A.; Jenekhe, S. A. *Chem. Mater.* **1992**, *4*, 1282. (c) Dotrong, M.; Mehta, R.; Balchin, G. A.; Tomlinson,

R. C.; Sinsky, M.; Lee, C. Y. C.; Evers, R. C. *J. Polym. Sci., Part A* **1993**, *31*, 723.

(25) (a) Osaheni, J. A.; Jenekhe, S. A.; Perlstein, J. *Appl. Phys. Lett.* **1994**, *64*, 3112. (b) Osaheni, J. A.; Jenekhe, S. A.; Perlstein, J. *J. Phys. Chem.* **1994**, *98*, 12727. (c) Jenekhe, S. A.; Yi, S. *Adv. Mater.* **2000**, *12*, 1274.

(26) (a) Pang, H.; Vilela, F.; Skabara, P. J.; McDouall, J. J. W.; Crouch, D. J.; Anthopoulos, T. D.; Bradley, D. D. C.; de Leeuw, D.; Horton, P. N.; Hursthouse, M. B. *Adv. Mater.* **2007**, *19*, 4438. (b) Mamada, M.; Nishida, J.-I.; Tokito, S.; Yamashita, Y. *Chem. Lett.* **2008**, *37*, 766. (c) McEntee, G. J.; Vilela, F.; Skabara, P. J.; Anthopoulos, T. D.; Labram, J. G.; Tierney, S.; Harrington, R. W.; Clegg, W. *J. Mater. Chem.* **2011**, *21*, 2091.

(27) (a) Mike, J. F.; Inteman, J. J.; Ellern, A.; Jeffries-EL, M. *J. Org. Chem.* **2010**, *75*, 495. (b) Mike, J. F.; Nalwa, K.; Makowski, A. J.; Putnam, D.; Tomlinson, A. L.; Chaudhary, S.; Jeffries-EL, M. *Phys. Chem. Chem. Phys.* **2011**, *13*, 1338. (c) Intemann, J. J.; Mike, J. F.; Cai, M.; Sayantan, B.; Xiao, T.; Mauldin, T. C.; Roggers, R. A.; Shinar, J.; Shinar, R.; Jeffries-EL, M. *Macromolecules* **2011**, *44*, 248.

(28) (a) Kulkarni, A. P.; Tonzola, C. J.; Babel, A.; Jenekhe, S. A. *Chem. Mater.* **2004**, *16*, 4556. (b) Agrawal, A. K.; Jenekhe, S. A. *Chem. Mater.* **1996**, *8*, 579.

(29) (a) Pope, M.; Swenberg, C. E. *Electronic Process in Organic Crystals and Polymers*, 2nd ed.; Oxford University Press: New York, 1999. (b) Arkhipov, V. I.; Bassler, H. *Phys. Status Solid A* **2004**, *201*, 1152.

(30) (a) Brabec, C. J.; Cravino, A.; Meissner, D.; Sariciftci, N. S.; Fromherz, T.; Rispens, M. T.; Sanchez, L.; Hummelen, J. C. *Adv. Funct. Mater.* **2001**, *11*, 374. (b) Gadisa, A.; Svensseon, M.; Andersson, M. R.; Inganäs, O. *Appl. Phys. Lett.* **2004**, *84*, 1609. (c) Potscavage, W. J.; Sharma, A.; Kippelen, B. *Acc. Chem. Res.* **2009**, *42*, 1758. (d) Perez, M. D.; Borek, C.; Forrest, S. R.; Thompson, M. E. *J. Am. Chem. Soc.* **2009**, *131*, 9281. (e) Brédas, J.-L.; Norton, J. E.; Cornil, J.; Coropceanu, V. *Acc. Chem. Res.* **2009**, *42*, 1691.

(31) Lee, J. K.; Ma, W. L.; Brabec, C. J.; Yuen, J.; Moon, J. S.; Kim, J. Y.; Lee, K.; Bazan, G. C.; Heeger, A. J. *J. Am. Chem. Soc.* **2008**, *130*, 3619.